cancer who received radiation therapy and 1,438 unrelated subjects. Consequently, the genotypes of 3,144 SNPs covering 494 genes were determined. The genes investigated in this study are listed in Table 1. To obtain accurate results in this case-control study, SNPs that departed from Hardy-Weinberg equilivbrium or that had a low minor allele frequency were excluded from further examination. Consequently, 2,651 SNPs were chosen for further analysis. The accuracy of the genotyping was tested by comparing the genotypes determined using the Invader assay with those determined using a RFLP analysis. More than 1,000 genotypes were assayed in three randomly chosen SNP loci. No genotypes showed any discrepancies between the two methods, indicating that the Invader assay had produced highly accurate genotypes (data not shown).

Identification of SNPs associated with radiation dermatitis. As a result of the screening steps described above, two loci were found to be associated with an adverse effect: the *IL12RB2* gene locus and the *ABCA1* gene locus. At the *IL12RB2* locus, 13 SNPs were examined (Supplementary Table S1). Among them, five SNPs were associated with radiation dermatitis (Table 3A). The strongest association was observed at SNP-K (rs3790568) in recessive model ($P = 0.0065$). To test the possibility that known coding SNPs mapped to the *IL12RB2* gene were associated with radiation dermatitis, we searched a dbSNP database and found six coding SNPs (rs2307146, rs7526769, rs2307148, rs2307145, rs2307153, and rs2307154). The genotypes of these coding SNPs were determined, but all the patients were wild-type (data not shown). At the *ABCA1* locus, 50 SNPs were analyzed (Supplementary Table S2); 8 SNPs were associated with radiation dermatitis, and the lowest P value of which was 0.0013 for SNP-17 (rs2253304) in allele frequency model (Table 3B). No other locus was associated with radiation dermatitis.

Haplotype block structure of IL12RB2 *and* ABCA1 *gene loci.* To narrow down the loci associated with radiation dermatitis, the haplotype block structures of both genes were estimated. The haplotypes and diplotypes of 13 SNPs at the *IL12RB2* locus were estimated in 1,594 unrelated individuals. Using the diplotypes of these individuals, the haplotype block structure of the *IL12RB2* locus was estimated using AdBlock software. Consequently, the 13 SNPs at the *IL12RB2* locus were subdivided into three haplotype blocks. All the SNPs associated with an adverse effect were located in the second haplotype block (Supplementary Table S1). As for the *ABCA1* gene, haplotype block analysis of the *ABCA1* gene revealed that the locus was subdivided into seven haplotype blocks. The SNPs

Table 2. Summary of patient characteristics and therapeutic variable

	Dermatitis group	Control group	P
Age (y)			
Median (range)	48 (30-73)	48 (23-77)	NS
Menopausal state			
Premenopausal	48	51	NS
Postmenopausal	29	28	
pT			
1	46	50	NS
2	31	28	
3	0	1	
pN			
0	58	67	NS
1	19	12	
Surgery			
Quadrantectomy	16	15	NS
Wide excision	61	64	
Surgery-radiotherapy interval (d)			
Median (range)	28 (10-123)	30 (3-233)	NS
Radiation source			
^{60}Co γ-rays	22	30	NS
4 MV X-rays	38	34	
6 MV X-rays	17	15	
Total radiation dose to whole breast (Gy)			
Median (range)	50 (44-52)	50 (44-52)	NS
Treatment time for whole-breast radiotherapy (d)			
Median (range)	36 (29-48)	36 (25-51)	NS
Dose per fraction (Gy)			
Median (range)	2.0 (1.8-2.2)	2.0 (1.8-2.2)	NS
Accumulative radiation dose per week (Gy/wk)			
Median (range)	9.6 (6.6-10.8)	9.6 (6.9-12.3)	NS
Concurrent tamoxifen			
Yes	39	54	0.024
No	38	25	
Concurrent oral fluorouracil			
Yes	25	32	NS
No	52	47	
Total	77	79	

Abbreviation: NS, not significant.

Table 3. Association between genes and radiation dermatitis

SNP name	Genotype	Dermatitis group	Control group	P	Odds ratio (95% CI)
A. Association between IL12RB2 and radiation dermatitis					
SNP-H (rs3790566)	CC	48	32	0.0065	2.45 (1.23-4.97)
	CT and TT	28	46		
SNP-I (rs379056)	GG	49	32	0.0062	2.50 (1.25-5.06)
	AG and AA	28	46		
SNP-K (rs3790568)	GG	51	34	0.0060	2.52 (1.26-5.13)
	AG and AA	26	44		
B. Association between ABCA1 and radiation dermatitis					
SNP-15 (rs2230806)	AA	13	29	0.0014	2.91 (1.30-6.78)
	AG and GG	63	48		
SNP-17 (rs2253304)	TT	13	29	0.0013	3.02 (1.35-7.04)
	CT and CC	64	47		
SNP-13 (rs2487058)	AA	13	28	0.0025	2.83 (1.26-6.67)
	AG and GG	61	46		

Abbreviation: 95% CI, 95% confidence interval.

associated with an adverse effect were located in the third and fifth haplotype blocks (Supplementary Table S2).

Estimation of the probability of radiation dermatitis for combined genotypes. To assess the probability of radiation dermatitis precisely, the genotypes of the two loci were used in a logistic regression model to estimate the probability of radiation dermatitis. Model selection using Akaike information criterion selected the best pair of SNPs, which consisted of SNP-15 in ABCA1 and SNP-K in IL12RB2. These analyses revealed that the genotype combination of a G homozygote at both SNP-15 and SNP-K exhibited the highest probability (0.75) of developing radiation-induced dermatitis (Table 4). This result indicates that 75% of patients carrying the combination of genotype have a chance to develop radiation-induced dermatitis. The genotype frequencies of these two SNPs were estimated based on genotyping data from 1,594 unrelated individuals. Based on these results, the frequency of the genotype with the highest probability of radiation dermatitis was estimated to be 0.147 in the Japanese population (Table 4).

Discussion

In this study, we showed associations between polymorphisms in the *IL12RB2* and *ABCA1* loci and an adverse effect in patients who received radiation therapy after undergoing surgery for breast cancer. SNPs associated with radiation dermatitis were observed in one or two of the haplotype blocks of the *IL12RB2* or *ABCA1* genes, respectively. These observations indicated that the associations between the SNPs and the adverse effect were nonrandom events.

Interleukin-12 (IL-12) receptor is a heterodimer protein consisting of two subunits: IL12RB1 and IL12RB2 (14). Several studies have shown that IL12RB2 may regulate IL-12 function (15). On the other hand, the cytokine IL-12 shows a wide variety of biological activities both *in vitro* and *in vivo*. Several studies have shown the antitumor activity of IL-12 through an effect on the host immune system. Schwarz et al. (16) reported that IL-12 suppresses UV radiation-induced apoptosis. IL-12 also prevents immunosuppression caused by UV irradiation. They concluded that IL-12 induces the expression of genes involved in nucleotide excision repair and that the activated nucleotide excision repair system may protect UV-irradiated cells from undergoing apoptosis. In their report, IL-12 was unable to suppress apoptosis caused by γ-irradiation *in vitro*. However, the effect of IL-12 on γ-irradiated cells *in vivo* remains to be observed. Our results may suggest that changes in the genotype of SNPs in IL12RB2 may regulate the biological function of IL-12, causing differences in the biological response to ionizing radiation.

The association between radiation-induced dermatitis and polymorphisms in the *ABCA1* gene is rather unexpected because the *ABCA1* gene plays an essential role in the efflux of cholesterol to high-density lipoprotein. However, the *ABCA1* gene has also been shown to be involved in the engulfment of apoptotic cells. Hamon et al. (17) showed that the loss of ABCA1 function impaired the engulfment of cell corpses generated by apoptosis. This result also suggests that the functions of the ABCA1 gene product are linked to apoptosis. In our study, a coding SNP (SNP-15; rs2230806), in which the nucleotide polymorphisms cause an amino acid substitution from Lys to Arg at the 219th amino acid, was associated with radiation-induced dermatitis. Considering the link between the *ABCA1* gene and apoptosis, this amino acid substitution may influence apoptotic reactions caused by ionizing radiation, thereby influencing the degree of dermatitis that occurs.

Table 4. Probability of radiation dermatitis for each genotype

rs2230806 (ABCA1)	rs3790568 (IL12RB2)	
	GG	AG or AA
GG	0.75 (0.147)	0.527 (0.093)
AG or AA	0.558 (0.466)	0.314 (0.294)

NOTE: Numbers in parentheses indicate genotype frequency in the Japanese population.

Data interpretation. The patient selection policy of the present study was developed to minimize the problems that a multi-institutional case-control study is liable to suffer. This policy was characterized by the patient-to-patient matching selection to avoid intergroup bias, the photograph-based confirmation for grading dermatitis, and the dose distribution-based exclusion of radiotherapy-related confounding factors.

In spite of patient-to-patient matching for the major prognostic factors, the proportion of patients treated with concurrent tamoxifen therapy were significantly larger in the control group than in the radiation dermatitis group ($P = 0.024$). This difference was the only intergroup bias observed out of all the patient- and treatment-related factors. The clinical significance of concurrent tamoxifen therapy in radiotherapy-related toxicity is controversial. Several reports have shown an increased risk of pulmonary and breast fibrosis after concurrent treatment with tamoxifen therapy and radiotherapy (18, 19), whereas other reports did not show any risk (20). Furthermore, an *in vitro* experimental study showed that the radiosensitivity of hormone-dependent breast cancer cells might be reduced through the cytostatic effect of tamoxifen (21). However, no experimental or clinical studies have suggested a radioprotective effect of tamoxifen on hormone-independent normal cells, including lymphocytes or fibroblasts. Therefore, we suspect that this intergroup bias did not seriously affect the interpretation of the SNP data.

Clinical relevance. Many *ex vivo* prediction systems have been developed and evaluated in which various numbers of patients treated with radiotherapy were studied prospectively or retrospectively using cellular or molecular *ex vivo* assays of lymphocytes or fibroblasts, with acute or late adverse effects as the clinical end points. The results of studies comparing clinical and cellular radiosensitivity using colony assays, micronucleus assays, and comet assays were often suggested to be promising. However, as reviewed by Twardella and Chang-Claude (22), the clinical relevance of these predictive assays should be carefully evaluated, considering any possible bias that may arise from inappropriate settings of patient cohorts, poorly defined clinical end points, or contamination by confounding external factors.

Recently, several studies have been undertaken to evaluate the correlation between clinical radiosensitivity and SNPs (23–26). Mostly, SNPs in selected genes whose functions may modify radiation-related toxicity, such as *ATM*, *TGFB1*, and *XRCC1*, have been analyzed. For instance, Andreassen et al. (23) analyzed seven SNPs in five genes (*TGFB1*, *SOD2*, *XRCC1*, *XRCC3*, and *APEX*) using cultured fibroblasts obtained from 41 patients who had been treated with uniform postmastectomy radiotherapy. Their data indicated that five of the seven SNPs were significantly correlated with the occurrence of grade 3 s.c. fibrosis or grade 2 to 3 telangiectasia in the irradiated skin. They concluded that SNP analysis may have the potential to predict clinical radiosensitivity, particularly when multiple SNPs are analyzed.

By logistic regression analysis, probabilities of radiation-induced dermatitis were estimated on each combination of genotypes of two SNPs (rs3790568 and rs2230806). These analyses revealed that three patients in four patients carrying a specific combination of genotypes, G homozygote in two SNPs, develop radiation-induced dermatitis. Genotype frequency of combination of the SNPs was estimated as 0.147 in the Japanese population. Therefore, ~11% of Japanese are predicted to develop radiation-induced dermatitis. Considering incidence of radiation-induced dermatitis (5-10%), this number seems to be reasonable.

The present study featured a much more comprehensive SNP analysis than any other previous study. At least a considerable part of clinically observed hyperradiosensitivity may be regulated by the integration of multiple minor alterations in genetic function. Therefore, a comprehensive analysis, as was done in the present study, is most suitable for identifying radiosensitive populations of patients. These results may serve as preliminary data for the construction of personalized radiation therapy.

Disclosure of Potential Conflicts of Interest

No potential conflicts of interest were disclosed.

Acknowledgments

We thank the patients for participating in the study and Yusaku Wada, Yuko Kanto, and Kiyoko Ogawa for their technical assistance.

References

1. Hiraoka M, Mitsumori M, Kokubo M. The roles and controversies of radiation therapy in breast conserving therapy for breast cancer. Breast Cancer 1997;4:127–33.
2. Rosen EM, Fan S, Rockwell S, Goldberg ID. The molecular and cellular basis of radiosensitivity: implications for understanding how normal tissues and tumors respond to therapeutic radiation. Cancer Invest 1999;17:56–72.
3. Fujishiro S, Mitsumori M, Kokubo M, et al. Cosmetic results and complications after breast conserving therapy for early breast cancer. Breast Cancer 2000; 7:57–63.
4. Morgan JL, Holcomb TM, Morrissey RW. Radiation reaction in ataxia telangiectasia. Am J Dis Child 1968; 116:557–8.
5. Gotoff SP, Amirmokri E, Liebner EJ. Ataxia telangiectasia. Neoplasia, untoward response to x-irradiation, and tuberous sclerosis. Am J Dis Child 1967;114: 617–25.
6. Alter BP. Radiosensitivity in Fanconi's anemia patients. Radiother Oncol 2002;62:345–7.
7. Burnet NG, Peacock JH. Normal cellular radiosensitivity in an adult Fanconi anaemia patient with marked clinical radiosensitivity. Radiother Oncol 2002;62: 350–1; author reply 1–2.
8. Distel L, Neubauer S, Varon R, Holter W, Grabenbauer G. Fatal toxicity following radio- and chemotherapy of medulloblastoma in a child with unrecognized Nijmegen breakage syndrome. Med Pediatr Oncol 2003;41: 44–8.
9. Tauchi H, Matsuura S, Kobayashi J, Sakamoto S, Komatsu K. Nijmegen breakage syndrome gene, NBS1, and molecular links to factors for genome stability. Oncogene 2002;21:8967–80.
10. Turesson I, Nyman J, Holmberg E, Oden A. Prognostic factors for acute and late skin reactions in radiotherapy patients. Int J Radiat Oncol Biol Phys 1996;36: 1065–75.
11. Hirakawa M, Tanaka T, Hashimoto Y, et al. JSNP: a database of common gene variations in the Japanese population. Nucleic Acids Res 2002;30:158–62.
12. Haga H, Yamada R, Ohnishi Y, Nakamura Y, Tanaka T. Gene-based SNP discovery as part of the Japanese Millennium Genome Project: identification of 190,562 genetic variations in the human genome. Single-nucleotide polymorphism. J Hum Genet 2002;47: 605–10.
13. Fujisawa H, Eguchi S, Ushijima M, et al. Genotyping of single nucleotide polymorphism using model-based clustering. Bioinformatics 2004;20:718–26.
14. Presky DH, Yang H, Minetti LJ, et al. A functional interleukin 12 receptor complex is composed of two β-type cytokine receptor subunits. Proc Natl Acad Sci U S A 1996;93:14002–7.
15. Rogge L, Barberis-Maino L, Biffi M, et al. Selective expression of an interleukin-12 receptor component by human T helper 1 cells. J Exp Med 1997;185: 825–31.
16. Schwarz A, Stander S, Berneburg M, et al. Interleu-

kin-12 suppresses ultraviolet radiation-induced apoptosis by inducing DNA repair. Nat Cell Biol 2002;4:26–31.
17. Hamon Y, Chambenoit O, Chimini G. ABCA1 and the engulfment of apoptotic cells. Biochim Biophys Acta 2002;1585:64–71.
18. Huang EY, Wang CJ, Chen HC, et al. Multivariate analysis of pulmonary fibrosis after electron beam irradiation for postmastectomy chest wall and regional lymphatics: evidence for non-dosimetric factors. Radiother Oncol 2000;57:91–6.
19. Bentzen SM, Skoczylas JZ, Overgaard M, Overgaard J. Radiotherapy-related lung fibrosis enhanced by tamoxifen. J Natl Cancer Inst 1996;88:918–22.
20. Pierce LJ, Hutchins LF, Green SR, et al. Sequencing of tamoxifen and radiotherapy after breast-conserving surgery in early-stage breast cancer. J Clin Oncol 2005;23:24–9.
21. Wazer DE, Tercilla OF, Lin PS, Schmidt-Ullrich R. Modulation in the radiosensitivity of MCF-7 human breast carcinoma cells by 17B-estradiol and tamoxifen. Br J Radiol 1989;62:1079–83.
22. Twardella D, Chang-Claude J. Studies on radiosensitivity from an epidemiological point of view—overview of methods and results. Radiother Oncol 2002;62:249–60.
23. Andreassen CN, Alsner J, Overgaard M, Overgaard J. Prediction of normal tissue radiosensitivity from polymorphisms in candidate genes. Radiother Oncol 2003;69:127–35.
24. Angele S, Romestaing P, Moullan N, et al. ATM haplotypes and cellular response to DNA damage: association with breast cancer risk and clinical radiosensitivity. Cancer Res 2003;63:8717–25.
25. Severin DM, Leong T, Cassidy B, et al. Novel DNA sequence variants in the hHR21 DNA repair gene in radiosensitive cancer patients. Int J Radiat Oncol Biol Phys 2001;50:1323–31.
26. Fernet M, Hall J. Genetic biomarkers of therapeutic radiation sensitivity. DNA Repair (Amst) 2004;3:1237–43.

Radiotherapy and Oncology 87 (2008) 418–424
www.thegreenjournal.com

Organ motion

Real-time tumor-tracking radiotherapy for adrenal tumors

Norio Katoh[a,*], Rikiya Onimaru[a], Yusuke Sakuhara[a], Daisuke Abo[a], Shinichi Shimizu[a], Hiroshi Taguchi[a], Yoshiaki Watanabe[a], Nobuo Shinohara[b], Masayori Ishikawa[c], Hiroki Shirato[a]

[a]Department of Radiology, and [b]Department of Renal and Genitourinary Surgery, Hokkaido University Graduate School of Medicine, Sapporo, Japan, [c]Department of Medical Physics, Hokkaido University Hospital, Sapporo, Japan

Abstract

Purpose: **To investigate the three-dimensional movement of internal fiducial markers near the adrenal tumors using a real-time tumor-tracking radiotherapy (RTRT) system and to examine the feasibility of high-dose hypofractionated radiotherapy for the adrenal tumors.**

Materials and methods: **The subjects considered in this study were 10 markers of the 9 patients treated with RTRT. A total of 72 days in the prone position and 61 treatment days in the supine position for nine of the 10 markers were analyzed. All but one patient were prescribed 48 Gy in eight fractions at the isocenter.**

Results: **The average absolute amplitude of the marker movement in the prone position was 6.1 ± 4.4 mm (range 2.3–14.4), 11.1 ± 7.1 mm (3.5–25.2), and 7.0 ± 3.5 mm (3.9–12.5) in the left–right (LR), craniocaudal (CC), and anterior–posterior (AP) directions, respectively. The average absolute amplitude in the supine position was 3.4 ± 2.9 mm (0.6–9.1), 9.9 ± 9.8 mm (1.1–27.1), and 5.4 ± 5.2 mm (1.7–26.6) in the LR, CC, and AP directions, respectively. Of the eight markers, which were examined in both the prone and supine positions, there was no significant difference in the average absolute amplitude between the two positions. No symptomatic adverse effects were observed within the median follow-up period of 16 months (range 5–21 months). The actuarial freedom-from-local-progression rate was 100% at 12 months.**

Conclusions: **Three-dimensional motion of a fiducial marker near the adrenal tumors was detected. Hypofractionated RTRT for adrenal tumors was feasible for patients with metastatic tumors.**

Keywords: Adrenal gland; Kidney; Organ motion; Radiotherapy

In the management of metastatic adrenal tumors, adrenalectomy is often performed with the intent to improve survival [5,9,11,12,14–17,19], even though its complication rates have been found to be 9–20% [5,9,11,12,14,15,19] and radiotherapy for adrenal metastases is usually chosen as a palliative option. Since the adrenal gland is located near organs such as the stomach, duodenum, kidney, and liver, it has been thought to be difficult to deliver sufficient doses to adrenal tumors. Rigorous accounting of organ motion may be necessary to ensure accurate radiotherapy of the adrenal gland so that an adequate dose for tumor control can be provided. Although several articles have been published regarding the measurement of renal mobility [1,2,4,29], to the best of our knowledge there are no data on organ motion in the adrenal/perirenal region. We have developed a method of inserting a fiducial marker near the adrenal gland and have used a real-time tumor-tracking radiotherapy (RTRT) system to investigate the three-dimensional movement of markers near the adrenal tumors in the supine and prone patient positions. The feasibility of high-dose hypofractionated radiotherapy for adrenal tumors was also clinically investigated.

Materials and methods

The RTRT system has already been described in detail in other literature [21–23]. In brief, the process for synchronizing the tracking of a marker with irradiation was as follows. Before treatment, a 2-mm gold marker was implanted near the tumor by means of image-guided procedures under local anesthesia, principally within 5 cm from the center of the gross tumor volume (GTV). Fig. 1 shows a representative case. After the insertion of the fiducial marker, multidetector-row CT with a slice thickness and an interval of 2 mm was performed in patient positions as the patient held his breath at the end of expiration, the point at which our previous research showed that gating efficiency was highest [20]. The fluoroscopic RTRT system

0167-8140/$ - see front matter doi:10.1016/j.radonc.2008.03.013

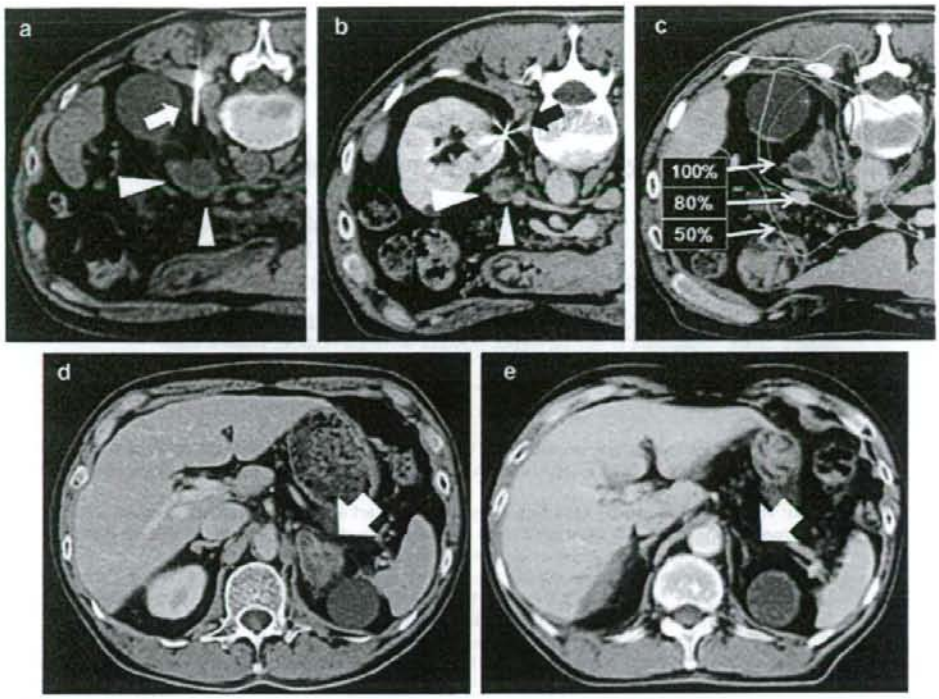

Fig. 1. Patient (No.8) with the left adrenal metastatic tumor treated with RTRT. There was an incidental left renal cyst near the tumor. (a) The fiducial gold marker was implanted near the left adrenal tumor (arrowhead) using a percutaneous approach. The 18-Gauge needle used for gold marker implantation (arrow) is visible in the CT image. (b) Implanted gold marker (arrow) was seen near the left adrenal tumor (arrowhead). (c) Radiation treatment plan. Red line showed 100% isodose line, aqua line 80%, and orange line 50%. (d) Tumor (arrowhead) as seen before RTRT. (e) Tumor had disappeared 12 months after RTRT with dose of 48 Gy in eight fractions.

consists of four sets of diagnostic fluoroscopic, image-processor units, a trigger-control unit, an image-display unit, and a conventional linear accelerator with multileaf collimators. Using two of the four fluoroscopy image-processor units, the system determines the three-dimensional position of the gold marker (2 mm in diameter) 30 times per second by using real-time pattern recognition and calibrated projection geometry. To avoid blocking the fluoroscopic images with the gantry of the linear accelerator, any two of the four X-ray systems can be selected. The linear accelerator is triggered to irradiate the tumor only when the gold marker is located within 2.0 mm of the planned coordinates relative to the isocenter in the lateral, craniocaudal, and anterior–posterior directions. The process of image acquisition and processing causes a small delay of 0.09 s between the marker recognition and the start of irradiation. A correction algorithm predicts the marker position from the speed of the marker movement, compensating for this delay.

Patients with metastatic adrenal tumors were candidates for RTRT if they were refractory to chemotherapy, or not eligible for surgery or chemotherapy. We included patients with perirenal metastatic lymphnodes as well as patients with adrenal tumors in this study. They were required to have a Karnofsky performance status of 70% or more and were excluded if their life expectancies were six months or less. Written informed consent was obtained from all patients before the treatment was initiated.

The subjects considered in this study were 9 male patients from October 2004 to September 2006. The median age was 66 years old (range 55–79 years old). Five of these patients had right-sided adrenal tumors, two had left-sided adrenal tumors, one patient had both-sided tumors, and one patient had a paraaortic node near the left adrenal gland, for a total of 10 tumors (Table 1). Each tumor had one fiducial marker, and so 10 markers in 9 patients were analyzed. All of the tumors were clinically diagnosed as metastatic tumors by computed tomography (CT) and/or positron emission tomography (PET). One patient with a left-sided adrenal tumor simultaneously had a renal tumor at the upper pole of the left kidney that was clinically diagnosed as renal cell carcinoma by CT. This patient was treated with RTRT for both tumors using a single fiducial marker at the perirenal region.

Table 1
Patient characteristics, the marker identifier, and clinical results of high-dose hypofractionated radiotherapy for adrenal tumors

Patient No.	Marker	Age	KPS	Tumor site	Primary cancer	Maximum diameter of GTV (cm)	Dose/fraction	Follow-up time (months)	Local tumor response	Status at the last follow-up
1	a	66	90	Left adrenal gland	Lung small cell carcinoma	5.5	48 Gy/8 Fr	16	SD	Dead
2	b	74	80	Right adrenal gland	Lung adenocarcinoma	3.5	48 Gy/8 Fr	21	CR (right)	Dead
2	c	–	–	Left adrenal gland	–	4.0	48 Gy/8 Fr	17	CR (left)	
3	d	55	90	Paraaortic lymphnode near left adrenal gland	HCC	3.0	30 Gy/8 Fr	19	CR	Dead
4	e	64	80	Right adrenal gland	Prostate adenocarcinoma	7.1	48 Gy/8 Fr	18	PR	Dead
5	f	79	90	Left adrenal gland	Lung adenocarcinoma	2.9	48 Gy/8 Fr	12	SD (adrenal)	Alive
5	f	–	–	Upper pole of left kidney	RCC	2.2	48 Gy/8 Fr		PR (renal)	
6	g	72	90	Right adrenal gland	Lung adenocarcinoma	2.0	48 Gy/8 Fr	13	CR	Alive
7	h	55	90	Right adrenal gland	HCC	8.0	48 Gy/8 Fr	5	SD	Dead
8	i	67	90	Left adrenal gland	Lung adenocarcinoma	6.0	48 Gy/8 Fr	18	CR	Dead
9	j	78	70	Left adrenal gland	Lung adenocarcinoma	6.5	48 Gy/8 Fr	3	SD	Dead

Abbreviations: No., number; KPS, Karnofsky performance status; GTV, gross tumor volume; HCC, hepatocellular carcinoma; RCC, renal cell carcinoma; CR, complete response; PR, partial response; SD, stable disease; Fr, fraction.

Multidetector-row CT was performed in both the prone and supine patient positions in this study. We have adopted the prone position in our protocol to reduce the dose to the stomach and duodenum. Eight of the 9 patients tolerated the protocol, but 1 patient complained of shortness of breath and was treated in the supine position. Patients were required to refrain from food for 4 h or more before the CT scan and actual treatment to keep the stomach and duodenum in a similar condition. Computed tomography was taken every three treatment days during the 2-week treatment period before the actual irradiation due to the possibility of the migration of the marker.

In this study, we investigated the difference between prone position and supine position in the trajectory of the marker and in the distance from the surface of the tumor to the stomach and duodenum. The coordinates of the gold marker implanted in the perirenal region were tracked continuously and recorded automatically to a hard disc every 0.033 s during RTRT in the prone treatment position for 1–2 min. Subsequently, the patient was moved to the supine position, and the marker was tracked for 1–2 min so that movement data could be acquired while in this position. Patients were not immobilized in either position. Each patient was treated with eight fractions for their tumors. A total of 72 treatment days for nine of the 10 markers in the prone position and 61 treatment days for nine of the 10 markers in the supine position were properly recorded. The absolute amplitudes of marker movement were defined as the distance between the maximum and minimum coordinates along each of the axes (left–right, craniocaudal, and anterior–posterior direction) in each log file [24]. Variations in amplitude among patients and also among treatment days for the same patient were examined. The movements observed in the different positions were compared in eight markers and the amplitudes of these movements were examined in each position. The minimum distance between the surface of the tumor and the stomach and duodenum was measured using the axial images of planning CT scans performed both in the prone and in the supine positions. The difference was evaluated using a paired or an unpaired *t* test according to the subject. $P < 0.05$ was considered statistically significant.

Clinical target volume (CTV) was defined as the GTV on CT with a 3-mm margin three-dimensionally. Planning target volume (PTV) was defined as CTV plus a 5-mm margin three-dimensionally with optimal reduction near the stomach and duodenum.

In principle, a dose of 48 Gy in eight fractions in 2 weeks was prescribed at the isocenter with the dose in the PTV greater than 80% of the isocenter dose. This dose fractionation schedule had been commonly used in RTRT for liver tumors [27]. One patient (No. 3) was treated with 30 Gy in eight fractions because he had a history of abdominal irradiation with 30 Gy in 10 fractions adjacent to the PTV in the present study. The dose–volume constraint for the stomach and duodenum was that 1 ml or less would receive 35 Gy in eight fractions, which is equivalent to 52 Gy using a daily fraction of 2 Gy (52 Gy/2 Gy) assuming an α/β ratio of 3 for late injury. As long as the contralateral kidney had sufficient enhancement on the CT image with a normal serum creatinine level, half of the ipsilateral renal volume was al-

lowed to be given 20 Gy in eight fractions, which is equivalent to 22 Gy/2 Gy assuming an α/β ratio of 3 for late injury.

The patients were seen and examined by one or two of the investigating physicians every 1–3 months. This evaluation included a physical examination, laboratory evaluation, and CT scan.

Disease progression was evaluated using the Response Evaluation Criteria in Solid Tumors (RECIST criteria) [28]. Local failure was defined as progression of the treated tumor. Adverse events were scored according to the National Cancer Institute Common Terminology Criteria for Adverse Events, version 3.0. In 2 patients, one who had bilateral tumors and another who underwent surgical removal of the opposite adrenal gland aldosteronoma 14 years before RTRT, we examined the adrenal hormonal level at rest before the treatment and every three months. The Kaplan–Meier method was used to calculate the actuarial rates of overall survival (OS) and freedom from local progression (FFLP), from the first day of radiotherapy.

Results

In the procedure of marker insertion, there was no patient who experienced symptomatic complications. Positions of the 10 markers are shown in Figs. 2 and 3. No further adverse effects related to the inserted markers were observed. There was no apparent migration or dislocation of the markers between the planning CT image and the CT images taken during the treatment period.

The average absolute amplitude of the marker movement in the prone position was 6.1 ± 4.4 mm (range 2.3–14.4), 11.1 ± 7.1 mm (range 3.5–25.2), and 7.0 ± 3.5 mm (range 3.9–12.5) in the left–right (LR), craniocaudal (CC), and anterior–posterior (AP) directions, respectively (Table 2). The average absolute amplitude in the supine position was 3.4 ± 2.9 mm (range 0.6–9.1), 9.9 ± 9.8 mm (range 1.1–27.1), and 5.4 ± 5.2 mm (range 1.7–26.6) in the LR, CC, and AP directions, respectively (Table 2). The average absolute amplitude was found to be significantly smaller in the LR direction compared to the CC direction ($p = 0.0364$) and AP direction ($p = 0.0441$) in the supine position.

Relationships between the average absolute amplitude and patient position and marker location are shown in Table 3. There was no statistically significant difference in the average absolute amplitude between the supine and prone positions along the three axes. Irrespective of patient position, no statistically significant difference in the average absolute amplitude was found between the left and right perirenal regions.

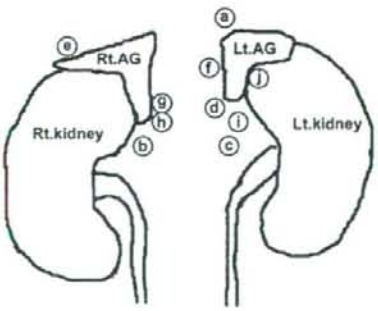

Fig. 2. A front view of the positions of 10 markers inserted in the perirenal region in 9 patients. AG, adrenal gland.

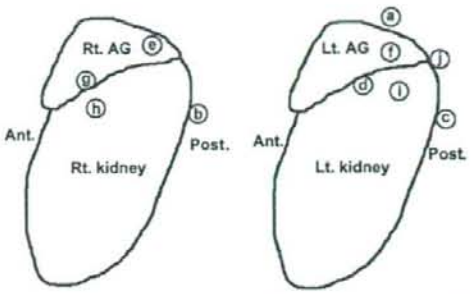

Fig. 3. A lateral view of the positions of 10 markers inserted in the perirenal region in 9 patients. AG, adrenal gland.

The minimum distances between the tumor and the stomach and duodenum are shown in Table 4. The averages of the minimum distances were 16.3 ± 21.5 mm and 17.6 ± 24.8 mm in the prone and supine positions, respectively. There were no significant differences in the mean minimum distances between the supine position and the prone position.

The volume of stomach and duodenum, which received 35 Gy or more, and the maximum dose at the stomach and duodenum are shown in Table 4. All the tumors were treated without violation in the dose constraint in the protocol except in one patient (No. 9) who had a left adrenal tumor attached to the gastric wall. His volume of the stomach and duodenum which received 35 Gy or more was larger than 1 ml. No patient complained of acute gastrointestinal adverse effects. In 2 patients, whose adrenal hormonal levels were examined at rest before the treatment and 7 and 11 months after the treatment, respectively, there was no decline in hormonal level. No other symptomatic adverse effects were observed within the median follow-up period of 16 months (range 5–21 months) in 9 patients. One patient (No. 9) who complained of tumor-related flank pain had experienced improvement of the pain after RTRT. All other patients without any tumor-related symptoms before RTRT showed no tumor-related symptoms after their treatment. By the time of the last follow-up, 7 patients had died. There were five tumors that showed a complete response, two with a partial response, and four with stable disease according to RECIST criteria (Table 1). The actuarial OS and FFLP rates at 12 months were 78% and 100%, respectively.

Discussion

Although there have been several articles regarding renal mobility [1,2,4,7,29] the three-dimensional movement of the adrenal gland or perirenal region has not yet been

Table 2
Average absolute amplitude of the marker for each patient

Marker	Average absolute amplitude ± SD (mm)							
	Prone position				Supine position			
	N[a]	LR	CC	AP	N[a]	LR	CC	AP
a	8	11.3 ± 9.6	25.2 ± 10.5	10.7 ± 13.0	8	9.1 ± 2.6	27.1 ± 12.1	14.2 ± 2.1
b	8	3.5 ± 1.9	4.2 ± 1.0	3.9 ± 1.3	3	1.3 ± 0.2	3.0 ± 0.9	1.8 ± 0.1
c	8	3.3 ± 1.1	13.0 ± 2.8	5.0 ± 1.4	8	3.5 ± 1.6	6.4 ± 3.1	2.2 ± 1.4
d	8	2.5 ± 1.5	3.5 ± 1.1	5.4 ± 2.7	8	0.6 ± 0.1	1.2 ± 0.1	0.7 ± 0.1
e	8	2.6 ± 0.7	17.9 ± 5.4	4.0 ± 0.7	8	3.5 ± 1.7	22.7 ± 4.7	6.6 ± 1.8
f	8	7.4 ± 4.3	10.2 ± 4.5	11.4 ± 8.6	8	6.4 ± 8.3	8.2 ± 4.2	12.5 ± 19.6
g	8	14.4 ± 5.7	10.1 ± 10.2	12.5 ± 8.7	8	4.3 ± 3.9	16.2 ± 3.1	7.9 ± 4.1
h	8	2.3 ± 1.1	4.2 ± 1.4	4.7 ± 1.1	8	1.4 ± 0.2	3.0 ± 0.5	2.2 ± 0.4
i	8	7.7 ± 4.5	11.2 ± 6.6	5.2 ± 1.2	–	–	–	–
j	–	–	–	–	2	0.7 ± 0.4	1.1 ± 1.1	0.7 ± 0.2
Total[b]	72	6.1 ± 4.4	11.1 ± 7.1	7.0 ± 3.5	61	3.4 ± 2.9	9.9 ± 9.8	5.4 ± 5.2

Abbreviations: SD, standard deviation; LR, left–right; CC, cranio-caudal; AP, antero-posterior.
[a] The value of *N* represents the number of treatment days which were properly recorded.
[b] The average at "Total" was calculated as (the sum of the average of each patient)/(number of patients). The standard deviation at "Total" was the standard deviation for the average of each patient.

Table 3
Relationships between the average absolute amplitude and patient position and marker location

	Average absolute amplitude ± SD (mm)			
	N[a]	LR	CC	AP
Patient position				
Prone	64	5.9 ± 4.7 (0.117)	11.0 ± 7.6 (0.962)	7.2 ± 3.7 (0.328)
Supine	59	3.8 ± 2.9	11.0 ± 9.8	6.0 ± 5.1
Marker location in prone position				
Right	32	5.7 ± 5.8 (0.815)	9.1 ± 6.5 (0.496)	6.3 ± 4.2 (0.619)
Left	40	6.5 ± 3.6	12.6 ± 7.9	7.5 ± 3.2
Marker location in supine position				
Right	27	2.6 ± 1.5 (0.484)	11.2 ± 9.9 (0.734)	4.6 ± 3.1 (0.712)
Left	34	4.1 ± 3.7	8.8 ± 10.7	6.1 ± 6.7

Abbreviations as in Table 2.
[a] The value of *N* represents the sum of the number of treatment days which were properly recorded for each condition. Data in parentheses are the *p* values for patient position; prone or spine and for marker location; right or left.

Table 4
The minimum distance between the surface of tumor and the stomach/duodenum, the volume of stomach/duodenum, which received 35 Gy or more, and the maximum dose at the stomach and duodenum

Patient No.	Minimum distance (mm)		Stomach and duodenum	
	Prone position	Supine position	Volume received 35 Gy or more (ml)	Maximum dose (cGy)
1	30	30	0.0	2936
2	7 (right)	8 (right)	0.1	3970
2	55 (left)	68 (left)	0.0	1624
3	18	15	0.0	2158
4	0	0	0.4	4119
5	50	53	0.1	4018
6	3	2	<0.1[a]	3626
7	0	0	<0.1[a]	3628
8	0	0	0.0	3416
9	0	0	4.6	4335

[a] Less than 0.1 ml

reported. As far as we could survey, this is the first report of the three-dimensional movement of the adrenal/perirenal region measured in the prone and supine positions using internal fiducial markers. The present study can be the basis for the determination of the PTV margin of adrenal gland tumors.

Contrary to our expectation, there was no statistically significant difference in the average absolute amplitude between the supine and prone positions along the three axes (LR, CC, and AP). Also, there were no statistically significant differences in the distance between the tumor and the stomach and that between the tumor and the duodenum regardless of whether the patients were in the prone or supine position. Thus, instead of the prone position, we now use the supine position, which is more comfortable for patients. In fact, there seems to be a tendency for reduced marker motion for patients in supine position in 5 of 8 patients as shown in Table 2. Although *t*-tests showed negative results on 2D motion in our series, there might be some difference in a larger study or in more detailed 3D analysis.

There have been only a few series of radiation therapy for metastatic adrenal tumors [10,25,31]. Zeng et al. reported that 22 patients with adrenal metastases from hepatocellular carcinoma were treated with palliative radiation therapy (median dose of 50 Gy/25 fractions), and 13 of 14 patients who had pain related to adrenal tumors had complete or marked pain relief [31]. In the present study, one patient experienced improvement of the pain and all other patients without any tumor-related symptoms before RTRT showed no tumor-related symptoms after their treatment. Since our treatment requires only a one-night stay in the hospital followed by a 2-week treatment as an out-patient in principle, patients would be more comfortable receiving our treatment than receiving 50 Gy in 25 fractions.

Several articles, with larger number of patients, on adrenalectomy for metastatic adrenal tumors reported that a few of patients survived more than 5 years [5,11,12,14–17,19]. In our series, the longest follow-up time was as short as 21 months. Therefore, surgery still has an advantage in terms of the possibility for the long-term survival until we would have longer follow-up and show the similar findings.

When compared with open adrenalectomy, laparoscopic adrenalectomy is associated with less intraoperative blood loss, lower analgesic requirement, decreased convalescence, superior cosmesis, and lower post-operative complication rates [3,13,18]. Laparoscopic adrenalectomy is currently considered to be the procedure of choice for benign adrenal masses. Several retrospective studies also showed the possible application of laparoscopic adrenalectomy for solitary adrenal metastasis [5,9,11,15,17,19]. However, the use of laparoscopic adrenalectomy for adrenal metastasis is controversial [8,30]. Even though laparoscopic surgery is a less invasive procedure, perioperative complications, such as diaphragm injury, inferior epigastric injury, pancreatic fistula, wound infection and bleeding, have been reported [5,9,11,15,17,19]. It was reported that complication rates ranged from 9% to 13% in laparoscopic surgical series [5,9,11,15,19]. Moreover, there have been several case reports about port site recurrence after laparoscopic adrenalectomy for adrenal metastatic tumors [6,26]. Our results showed no symptomatic complications, and no adrenal relapses were experienced in the treatment of 11 tumors. Although the number of patients was too small to draw definitive conclusions, the present study suggested that our procedure would be a feasible alternative to surgical adrenalectomy for treating adrenal metastasis.

The drawback to fluoroscopic imaging throughout treatment is the additional patient dose. However, we have found that the dose was negligible in most of occasions and can be included in treatment planning if necessary [22]. We still do not have any experience with RTRT for benign adrenal tumors, which would also be a challenging procedure in patients who, for medical reasons, have a high risk of surgical complication.

In conclusion, hypofractionated RTRT was feasible for patients with metastatic adrenal tumors. The motion of a fiducial marker near the tumor was demonstrated using the RTRT system. The minimum distances between the tumor and the stomach and duodenum were 16.3 ± 21.5 mm and 17.6 ± 24.8 mm in the prone and supine positions, respectively, with no significant difference between the two.

Acknowledgement

This study was partly supported by grant-in-aid for scientific research from Japanese Ministry of Education, Culture, Sports, Science and Technology.

* **Corresponding author. Norio Katoh**, Department of Radiology, Hokkaido University Graduate School of Medicine, North-15 West-7, Kita-ku, Sapporo 060-8638, Japan. *E-mail address:* noriwo@radi.med.hokudai.ac.jp

Received 20 November 2007; received in revised form 17 March 2008; accepted 21 March 2008; Available online 23 April 2008

References

[1] Balter JM, Ten Haken RK, Lawrence TS, Lam KL, Robertson JM. Uncertainties in CT-based radiation therapy treatment planning associated with patient breathing. Int J Radiat Oncol Biol Phys 1996;36:167–74.

[2] Brandner ED, Wu A, Chen H, et al. Abdominal organ motion measured using 4D CT. Int J Radiat Oncol Biol Phys 2006;65:554–60.

[3] Brunt LM, Doherty GM, Norton JA, Soper NJ, Quasebarth MA, Moley JF. Laparoscopic adrenalectomy compared to open adrenalectomy for benign adrenal neoplasms. J Am Coll Surg 1996;183:1–10.

[4] Bussels B, Goethals L, Feron M, et al. Respiration-induced movement of the upper abdominal organs: a pitfall for the three-dimensional conformal radiation treatment of pancreatic cancer. Radiother Oncol 2003;68:69–74.

[5] Castillo OA, Vitagliano G, Kerkebe M, Parma P, Pinto I, Diaz M. Laparoscopic adrenalectomy for suspected metastasis of adrenal glands: our experience. Urology 2007;69:637–41.

[6] Chen B, Zhou M, Cappelli MC, Wolf Jr JS. Port site, retroperitoneal and intra-abdominal recurrence after laparoscopic acrenalectomy for apparently isolated metastasis. J Urol 2002;168:2528–9.

[7] Davies SC, Hill AL, Holmes RB, Halliwell M, Jackson PC. Ultrasound quantitation of respiratory organ motion in the upper abdomen. Br J Radiol 1994;67:1096–102.

[8] Gill IS. The case for laparoscopic adrenalectomy. J Urol 2001;166:429–36.

[9] Heniford BT, Arca MJ, Walsh RM, Gill IS. Laparoscopic adrenalectomy for cancer. Semin Surg Oncol 1999;16:293–306.

[10] Higashiyama M, Doi O, Kodama K, Yokouchi H, Imaoka S, Koyama H. Surgical treatment of adrenal metastasis following pulmonary resection for lung cancer: comparison of adrenalectomy with palliative therapy. Int Surg 1994;79:124–9.
[11] Kebebew E, Siperstein AE, Clark OH, Duh QY. Results of laparoscopic adrenalectomy for suspected and unsuspected malignant adrenal neoplasms. Arch Surg 2002;137:948–51.
[12] Kim SH, Brennan MF, Russo P, Burt ME, Coit DG. The role of surgery in the treatment of clinically isolated adrenal metastasis. Cancer 1998;82:389–94.
[13] Linos DA, Stylopoulos N, Boukis M, Souvatzoglou A, Raptis S, Papadimitriou J. Anterior, posterior, or laparoscopic approach for the management of adrenal diseases? Am J Surg 1997;173:120–5.
[14] Mercier O, Fadel E, de Perrot M, et al. Surgical treatment of solitary adrenal metastasis from non-small cell lung cancer. J Thorac Cardiovasc Surg 2005;130:136–40.
[15] Moinzadeh A, Gill IS. Laparoscopic radical adrenalectomy for malignancy in 31 patients. J Urol 2005;173:519–25.
[16] Porte H, Siat J, Guibert B, et al. Resection of adrenal metastases from non-small cell lung cancer: a multicenter study. Ann Thorac Surg 2001;71:981–5.
[17] Sarela AI, Murphy I, Coit DG, Conlon KC. Metastasis to the adrenal gland: the emerging role laparoscopic surgery. Ann Surg Oncol 2003;10:1191–6.
[18] Schell SR, Talamini MA, Udelsman R. Laparoscopic adrenalectomy for nonmalignant disease: improved safety, morbidity, and cost-effectiveness. Surg Endosc 1999;13:30–4.
[19] Sebag F, Calzolari F, Harding J, Sierra M, Palazzo FF, Henry JF. Isolated adrenal metastasis: the role of laparoscopic surgery. World J Surg 2006;30:888–92.
[20] Seppenwoolde Y, Shirato H, Kitamura K, et al. Precise and real-time measurement of 3D tumor motion in lung due to breathing and heartbeat, measured during radiotherapy. Int J Radiat Oncol Biol Phys 2002;53:822–34.
[21] Shirato H, Shimizu S, Kitamura K, et al. Four-dimensional treatment planning and fluoroscopic real-time tumor tracking radiotherapy for moving tumor. Int J Radiat Oncol Biol Phys 2000;48:435–42.
[22] Shirato H, Shimizu S, Kunieda T, et al. Physical aspects of a real-time tumor tracking system for gated radiotherapy. Int J Radiat Oncol Biol Phys 2000;48:1187–95.
[23] Shirato H, Shimizu S, Shimizu T, Nishioka T, Miyasaka K. Real-time tumour tracking radiotherapy. Lancet 1999;353:1331–2.
[24] Shirato H, Suzuki K, Sharp GC, et al. Speed and amplitude of lung tumor motion precisely detected in four-dimensional setup and in real-time tumor-tracking radiotherapy. Int J Radiat Oncol Biol Phys 2006;64:1229–36.
[25] Soffen EM, Solin LJ, Rubenstein JH, Hanks GE. Palliative radiotherapy for symptomatic adrenal metastases. Cancer 1990;65:1318–20.
[26] Suzuki K, Ushiyama T, Mugiya S, Kageyama S, Saisu K, Fujita K. Hazards of laparoscopic adrenalectomy in patients with adrenal malignancy. J Urol 1997;158:2227.
[27] Taguchi H, Sakuhara Y, Hige S, et al. Intercepting radiotherapy using a real-time tumor-tracking radiotherapy system for highly selected patients with hepatocellular carcinoma unresectable with other modalities. Int J Radiat Oncol Biol Phys 2007;69:376–80.
[28] Therasse P, Arbuck SG, Eisenhauer EA, et al. New guidelines to evaluate the response to treatment in solid tumors. European Organization for Research and Treatment of Cancer, National Cancer Institute of the United States, National Cancer Institute of Canada. J Natl Cancer Inst 2000;92:205–16.
[29] van Sörnsen de Koste JR, Senan S, Kleynen CE, Slotman BJ, Lagerwaard FJ. Renal mobility during uncoached quiet respiration: an analysis of 4DCT scans. Int J Radiat Oncol Biol Phys 2006;64:799–803.
[30] Wells SA, Merke DP, Cutler GB, Norton JA, Lacroix A. Therapeutic controversy: the role of laparoscopic surgery in adrenal disease. J Clin Endocrinol Metab 1998;83:3041–9.
[31] Zeng ZC, Tang ZY, Fan J, et al. Radiation therapy for adrenal gland metastases from hepatocellular carcinoma. Jpn J Clin Oncol 2005;35:61–7.

Int. J. Radiation Oncology Biol. Phys., Vol. ■, No. ■, pp. 1–5, 2009

0360-3016/09/$–see front matter

ELSEVIER

doi:10.1016/j.ijrobp.2008.11.026

CLINICAL INVESTIGATION

CLINICAL OUTCOMES OF STEREOTACTIC BODY RADIOTHERAPY FOR SMALL LUNG LESIONS CLINICALLY DIAGNOSED AS PRIMARY LUNG CANCER ON RADIOLOGIC EXAMINATION

TETSUYA INOUE, M.D.,* SHINICHI SHIMIZU, M.D.,* RIKIYA ONIMARU, M.D.,* ATSUYA TAKEDA, M.D.,† HIROSHI ONISHI, M.D.,† YASUSHI NAGATA, M.D.,‡ TOMOKI KIMURA, M.D.,‖ KATSUYUKI KARASAWA, M.D.,¶ TAKURO ARIMOTO, M.D.,# MASATO HAREYAMA, M.D.,** EIKI KIKUCHI, M.D.,†† AND HIROKI SHIRATO, M.D.*

*Hokkaido University Department of Radiology, Sapporo, Japan; †Ofuna Central Hospital, Department of Radiology, Ofuna, Japan; ‡Yamanashi University Department of Radiology, Kofu, Japan; §Hiroshima University Department of Radiology, Hiroshima, Japan; ‖Kagawa University Department of Radiology, Takamatsu, Japan; ¶Tokyo Metropolitan Komagome Hospital, Department of Radiology, Tokyo, Japan; #Kitami Red Cross Hospital, Department of Radiology, Kitami, Japan; **Sapporo Medical University Department of Radiology, Sapporo, Japan; and ††Hokkaido University First Department of Internal Medicine, Sapporo, Japan

Purpose: Image-guided biopsy occasionally fails to diagnose small lung lesions, which are highly suggestive of primary lung cancer. The aim of the present study was to evaluate the outcome of stereotactic body radiotherapy (SBRT) for small lung lesions that were clinically diagnosed as primary lung cancer without pathologic confirmation.
Methods and Materials: A total of 115 patients were treated with SBRT in 12 institutions. Tumor size ranged from 5 to 45 mm in diameter, with a median of 20 mm.
Results: The 3-year and 5-year overall survival rates for patients with a tumor size ≤20 mm in diameter ($n = 58$) were both 89.8%, compared with 60.7% and 53.1% for patients with tumors >20 mm ($n = 57$) ($p < 0.0005$), respectively. Local progression occurred in 2 patients (3.4%) with a tumor size ≤20 mm and in 3 patients (5.3%) with tumors >20 mm. Among the patients with a tumor size ≤20 mm, Grade 2 pulmonary complications were observed in 2 (3.4%), but no Grade 3 to 5 toxicity was observed. In patients with a tumor size >20 mm, Grades 2, 3, and 5 toxicity were observed in 5 patients (8.8%), 3 patients (5.3%), and 1 patient (1.8%), respectively.
Conclusion: In patients with a tumor ≤20 mm in diameter, SBRT was reasonably safe in this retrospective study. The clinical implications of the high local control rate depend on the accuracy of clinical/radiologic diagnosis for small lung lesions and are to be carefully evaluated in a prospective study. © **2009 Elsevier Inc.**

Lung cancer, Stereotactic radiotherapy, Stereotactic body radiotherapy.

INTRODUCTION

Pathologic diagnosis is essential for the treatment of primary lung cancer. However, image-guided biopsy occasionally fails to diagnose small lung lesions, which are highly suggestive of primary lung cancer. When patients refuse re-biopsy or surgical resection, watchful waiting is usually indicated. There are other groups of patients in whom a pathologic diagnosis is very difficult to make, such as those with medical reasons for not being able to undergo biopsy and those with a history of surgical resection of non–small-cell lung cancer (NSCLC) and a small peripheral lung lesion on follow-up computed tomography (CT). The patients in the latter group often have difficulty undergoing a second surgical resection because of lowered respiratory function resulting from the previous surgery. Patients with cancer who are under watchful waiting are at risk for invasive growth of the primary tumor, lymphatic spread, and distant metastasis. Patients who choose to receive elective surgical resection of the small lung lesions to quantify the pathologic diagnosis may experience serious respiratory dysfunction. A proportion of the patients who do not have malignant tumors are inevitably overtreated and experience surgical complications.

Stereotactic body radiotherapy (SBRT) has been one of the treatments for Stage I NSCLC in medically inoperable patients. Recently, high local control and survival rates of SBRT were

Reprint requests to: Hiroki Shirato, M.D., Ph.D., Department of Radiology, Hokkaido University Graduate School of Medicine, North 15 West 7, Kita-ku, Sapporo 060-8638, Japan. Tel: +81-11-706-5977; Fax: +81-11-706-7876; E-mail: hshirato@radi.med.hokudai.ac.jp

Conflict of interest: none.

Acknowledgments—This study was supported in part by the Ministry of Health, Labour, and Welfare and by the Ministry of Education, Culture, Sports, Science, and Technology, Japan.

Received Aug 21, 2008, and in revised form Nov 17, 2008. Accepted for publication Nov 20, 2008.

reported in several studies (1–7). Onishi *et al.* summarized the results of a Japanese series retrospectively and reported that a pulmonary complication rate of above Grade 2 arose in only 5.4% of patients (1). For the patients who received a dose compatible with the biologic effective dose (BED) of 100 Gy or more, the local control rate was 91.6%. For the patients who were judged to have been operable but who were treated with SBRT, the 5-year overall survival rate was 70.8%, which is equivalent to that achieved in the previously mentioned surgery series (1).

A serious question among radiation oncologists is whether it is ethically justifiable not to give SBRT to those patients who have peripheral lung lesions highly suggestive of lung cancer but who failed to have lung cancer diagnosed pathologically. If SBRT is as safe as image-guided re-biopsy and as effective as surgical resection, it may be ethical to give SBRT to these patients. However, we cannot answer this question, because the risk and benefit have not been compared between elective surgical resection, watchful waiting, and SBRT for small peripheral lung lesions without pathologic confirmation.

We have found in a national survey of SBRT that a small number of patients with the clinical diagnosis of NSCLC are actually treated with SBRT without pathologic confirmation in each institution. The aim of the present study was to evaluate the outcome of SBRT for peripheral small lung lesions that were clinically diagnosed as primary lung cancer without pathologic confirmation in 12 institutions during the past 10 years in Japan.

METHODS AND MATERIALS

Eligibility criteria

Twelve institutions were selected from the member institutions of the Japan Clinical Oncology Group trial, JCOG0403, for which the quality of clinical record and dosimetry accuracy of SBRT had already been evaluated by audit (8). This is a multi-institutional retrospective study using the same eligibility criteria, which were that (a) surgery was contraindicated or refused, (b) the tumor diameter was <50 mm, (c) tumors were highly suggestive of primary lung cancer and diagnosed as Stage I lung cancer clinically but the patients did not have a pathologic diagnosis, and (d) the performance status was 0 to 2 according to World Health Organization guidelines.

Patients

A total of 115 patients who were highly suspected of having lung cancer but who lacked pathologic confirmation of the disease were diagnosed with Stage I lung cancer clinically and treated with SBRT in 12 institutions during the last 10 years in Japan. The patient characteristics are given in Table 1. There were 93 cases of T1N0M0 and 22 cases of T2N0M0 disease. The number of medically operable and inoperable patients was 43 and 72, respectively. Tumor size was recorded at the maximum diameter on the CT scan taken at the start of radiotherapy. The median tumor size was 20 mm (range, 5–45 mm). The median follow-up period was 14 months (range, 1–142 months). There were 11 patients whose follow-up period was <4 months at the time of this analysis.

Diagnosis was based on CT findings and enlargement of the lesion on sequential examination with or without fluorodeoxyglucose (FDG)–positron emission tomography (PET) findings. The tumors were diagnosed as highly suggestive of primary lung cancer by diagnostic radiologists when there was definitive enlargement of the lesion on sequential CT examination and/or positive findings on FDG-PET without any metastatic lesion in the diagnostic evaluation. Several findings such as the configuration of the lung lesion were also used in the diagnosis. Of 72 patients who were examined with FDG-PET, 67 patients had positive findings on FDG-PET. Other clinical history and findings as well as laboratory findings were also used for diagnosis as much as possible to prevent inclusion of patients with metastatic lung tumors or inflammatory or granulomatous lesions in the study population.

Table 1. Characteristics of patients (115 patients)

Characteristic	Value
Age (y)	
Median	77
Range	50–92
Gender (*n*)	
Male	87
Female	28
Tumor size (mm)	
Median	20
Range	5–45
T stage (*n*)	
T1	93
T2	22
Medical condition (*n*)	
Operable	43
Inoperable	72

The reasons for the lack of pathologic confirmation were as follows: (a) bronchoscope- or CT-guided biopsy failed in 59 patients, and these patients refused re-biopsy or surgical resection; (b) 21 patients were not indicated for a biopsy procedure or surgery because of medical complications; (c) 14 patients refused a biopsy procedure as well as surgery even at the initial examination; (d) a biopsy was not indicated in 14 patients because their history of NSCLC was strongly suggestive of the new development of a second primary NSCLC, likely inoperable, and they refused surgery; and (e) a biopsy was not indicated in 7 patients because there was little possibility to confirm the pathology because of the tumor's small size, and these patients refused surgery.

Radiotherapy

All patients underwent irradiation using stereotactic techniques. Three-dimensional treatment planning was performed using non-coplanar static ports or dynamic arcs. Various techniques using breathing control or gating methods and immobilization devices such as a vacuum cushion with or without a stereotactic body frame were used to reduce respiratory internal margins. Appropriate margins were adopted for the clinical target volume and the planning target volume.

A total dose of 30 to 70 Gy at the isocenter was administered in two to 10 fractions. Using a linear-quadratic model, we defined the BED as $nd(1+d/\alpha/\beta)$, with Gray units, where n was the fractionation number, d was the daily dose, and the α/β ratio was assumed to be 10 for tumors. The BED was not corrected with values for tumor doubling time or treatment term. The median BED at the isocenter in this study was 106 Gy (range, 56–141 Gy).

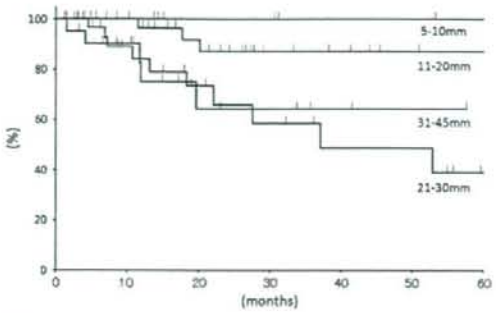

Fig. 1. Kaplan-Meier curve of overall survival rates for the patients with a tumor size (diameter) of 5 to 10 mm (n = 11), 11 to 20 mm (n = 47), 21 to 30 mm (n = 35), and 31 to 45 mm (n = 22).

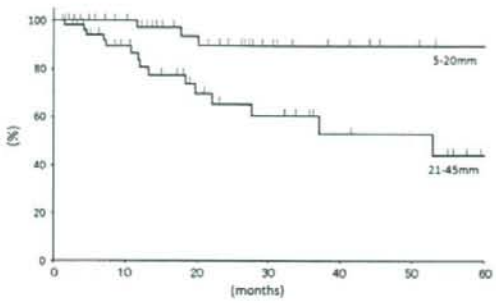

Fig. 2. Kaplan-Meier curve of overall survival rates for the patients with a tumor size (diameter) of 5 to 20 mm (n = 58) and 21 to 45 mm (n = 57). A statistically significant difference was found (p < 0.0005) between the two groups.

Ethical considerations

Use of SBRT was approved for Stage I lung cancer by the ethics committee in each institution. Clinically diagnosed Stage I lung cancer was not included in the ineligibility criteria at each institution. Written informed consent to receive SBRT was obtained from all patients. This retrospective study was approved by the ethics committee of each institution and was performed in accordance with the 1975 Declaration of Helsinki, as revised in 2000.

Statistical analysis

Overall survival rates were calculated from the first day of treatment using the Kaplan-Meier method. The log-rank test was used to calculate statistically significant differences. A value of $p < 0.05$ was considered to be statistically significant.

RESULTS

Survival

We separated the patients into four groups by tumor size at its maximum diameter, consisting of the 5 to 10 mm (Group A; n = 11), 11 to 20 mm (Group B; n = 47), 21 to 30 mm (Group C; n = 35), and 31 to 45 mm (Group D; n = 22) groups. The 3-year and 5-year overall survival rates were both 100% for Group A, both 87.2% for Group B, 58.7% and 48.9% for Group C, and both 64.5% for Group D (Fig. 1). When we excluded the 11 patients whose follow-up period was <4 months, there was no apparent difference in these results; 3-year and 5-year overall survival rates were both 100% for Group A, both 87.2% for Group B, and 58.7% and 39.2% for Group C, and both 67.7% for Group D.

The 3-year and 5-year overall survival rates were both 89.8% for patients with a tumor size ≤20 mm (n = 58) compared with 60.7% and 53.1% for patients with a tumor size >20 mm (n = 57) (p <0.0005; Fig. 2). According to medical operability, the 3-year and 5-year overall survival rates for operable patients (n = 43) were both 88.4%, compared with 67.0% and 60.9% for inoperable patients (n = 72) (Fig. 3). According to BED, the 3-year and 5-year overall survival rates for the patients with BED <100 Gy (n = 17) were both 71.8%, compared with 76.6% and 61.9% for the patients with BED ≥ 100 Gy (n = 98) (Fig. 4).

Local tumor response and distant metastases

Local progression occurred in 2 patients (3.4%) with a tumor size ≤20 mm and in 3 patients (5.3%) with a tumor size >20 mm. Lymphatic and distant metastasis were observed in 3 patients (5.2%) and 6 patients (10.3%) with a tumor size ≤20 mm and in 6 patients (10.5%) and 10 patients (17.5%) with a tumor size >20 mm, respectively. For the patients with BED <100 Gy, no local progression occurred.

Toxicities

Pulmonary adverse effects were graded according to the Common Toxicity Criteria for Adverse Events version 3.0. In brief, radiation pneumonitis was graded as follows: Grade 1, asymptomatic, radiologic findings only; Grade 2, symptomatic, not interfering with activities of daily life (ADL); Grade 3, interfering with ADL, O2 indicated; Grade 4, life-threatening, ventilatory support indicated; and Grade 5, death.

Of patients with a tumor size ≤20 mm in diameter, Grade 2 pulmonary complications were observed in 2 patients (3.4%), whereas no patients experienced Grade 3 to 5 toxicities. In patients with a tumor size >20 mm, Grades 2, 3, and 5 pulmonary toxicities were observed in 5 patients (8.8%), 3 patients (5.3%), and 1 patient (1.8%), respectively. A Grade 5 pulmonary complication occurred in 1 patient with interstitial pneumonia, which resulted in acute worsening from SBRT after 1.5 months. One case of radiation pleuritis, one case of intercostal neuralgia, and one case of rib fracture were observed, but these patients' symptoms were controlled easily by conservative treatment. Grade 2 pulmonary toxicity occurred in 3 cases (17.6%) in patients with BED <100 Gy and in 8 cases (8.2%) in patients with BED ≥100 Gy.

DISCUSSION

There is no doubt that pathologic diagnosis is the most accurate diagnosis for lung tumors. When possible, clinicians

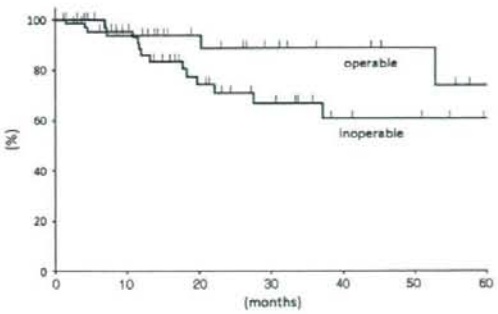

Fig. 3. Kaplan-Meier curve of overall survival rates for operable (n = 43) and inoperable (n = 72) patients. No statistically significant difference was found (p = 0.07) between two groups.

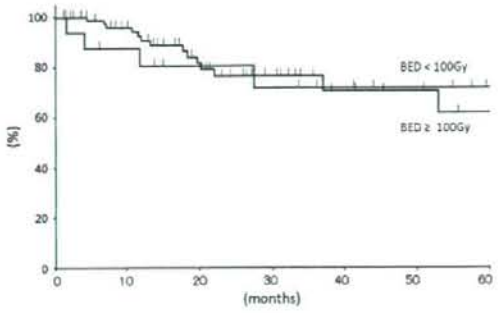

Fig. 4. Kaplan-Meier curve of overall survival rates for the patients with a biologic effective dose (BED) <100 (n = 17) and a BED ≥100 (n = 98). No statistically significant difference was found (p = 0.95) between the two groups.

should persuade patients to receive pathologic confirmation before SBRT and to receive surgical resection if they are operable. However, as we have observed in this retrospective study, for patients with poor respiratory function, pathologic confirmation of the small lung lesions is often difficult or life threatening and occasionally abandoned by pulmonologists and thoracic surgeons. Therefore, it is extremely important to find a subset of patients who would benefit from SBRT instead of the conventional strategy of watchful waiting or elective surgical resection.

In patients with clinically diagnosed lung cancer ≤20 mm in diameter, the 3-year survival rate was 89.8% in our series. Although the median follow-up is still short, the 5-year survival rate was projected to be 89.8% for these patients. Because of the very low complication rate for these patients, SBRT for inoperable patients highly likely to have Stage I lung cancer with tumors ≤20 mm in diameter may be justifiable. However, the excellent survival rates for those patients with tumors ≤20 mm may be partly caused by the inclusion of nonmalignant lesions in the radiation-treated patients. The clinical implications of the high local control rate depend on the accuracy of clinical/radiologic diagnosis for small lung lesions and are to be carefully evaluated in a prospective study.

Median follow-up period 14 months was relatively short, including 11 patients whose follow-up period was <4 months. However, 3- and 5-year survival data were not impacted so much by them because follow-up period of the other patients was much longer.

Onishi *et al.* reported that the patients treated with BED <100 Gy had a tendency to have worse clinical outcomes than those treated with larger dose in SBRT (1). In this study, there were only 17 patients who received BED <100 Gy. There was no significant difference in overall survival rates between those treated with BED <100 Gy and those treated with BED≥100Gy, probably because of the small number of the patients who received BED <100 Gy.

Improvement of clinical/radiologic diagnosis of small lung tumors is essential if SBRT is used for clinically diagnosed Stage I lung cancer. Before the introduction of FDG-PET, the percentage of benign diseases in the solitary lung nodules detected by plain chest X-ray or CT was reported to be 25% to 50%, which is obviously too high (9–12). However, improvement of imaging modalities has made it possible to diagnose small peripheral lung cancer much more precisely than before. There were recent reports that FDG-PET and PET/CT showed 88% to 96.8% sensitivity, 77% to 77.8% specificity, and 91.2% accuracy in diagnosis of primary lung cancer (13, 14). A combination of positive FDG-PET findings, enlargement of the nodule on CT image, and negative laboratory tests for worsening of inflammatory diseases would reduce the false-positive diagnosis of Stage I lung cancer. However, Nomori *et al.* reported that lung nodules that were <10 mm in size or that showed ground-glass opacity on CT image cannot be evaluated accurately by FDG-PET (15). Therefore, for solid round tumors ≤10 mm and those with ground-glass appearance, watchful waiting would be the preferable choice at present, and improvement in diagnostic imaging is warranted. In addition, even if small lung lesions are highly suggestive of primary lung cancer on clinical/radiologic examination, the possibility of small-cell lung cancer (SCLC), for which it is better to be given additional chemotherapy, cannot be excluded. Some tumor markers such as neuron-specific enolase or progastrin-releasing peptide are shown to have relatively high sensitivity and specificity for SCLC (16). Tumor marker screening has the potential to reduce the inclusion of SCLC, although the tumor size may be too small to detect marker elevation.

Recently video-assisted thoracoscopic surgery (VATS) for lung cancer has become a safe and common procedure. In comparison with open surgery, VATS is less invasive and is associated with less morbidity and mortality (17). However, a recent review showed that VATS still has a 3.3% to 13.4% complication rate for surgical biopsy and a 7.7% to 36.6% complications rate for lobectomy (17). In 567 patients with peripheral NSCLC ≤20 mm who were operable as evaluated by cardiopulmonary function tests and had no history of previously treated cancer, the complication rate was reported to be 6.6% for sublobar resection and 7.3% for lobar

resection with 1 operative death (18). In the present SBRT study, for patients with a peripheral lung tumor ≤20 mm who were often inoperable based on cardiopulmonary function tests and who could have a history of previously treated cancer, only 3.4% (2 of 58) experienced Grade 2 pulmonary complications and none experienced Grade 3 to 5 complications. Therefore, although the comparison of the complication between surgery and SBRT is difficult, SBRT can be regarded as a safer treatment than lobectomy using VATS and as safe as biopsy using VATS for patients with a tumor size ≤20 mm. On the contrary, for patients with a tumor size >20 mm, Grade 2, 3, and 5 pulmonary complications were observed in 8.8% (5 of 57), 5.3% (3 of 57), and 1.8% (1 of 57) of study patients, respectively. Because the risk of SBRT is not minimal for these patients, the indication of SBRT for clinically diagnosed Stage I lung cancer with a tumor >20 mm should be very carefully evaluated by members of the cancer board in each institution.

It is important to state that our study does not give any guidance for inoperable patients whose tumors are highly suggestive of benign lesions but that cannot be definitely determined not to be malignant, as this study looks only at those with tumors highly suggestive of malignant lesions. Patients with benign pulmonary lesion such as hamartoma, granulomatous inflammation, and focal fibrosis may require pathologic confirmation because these patients sometimes have tumors highly suggestive of benign lesions but that cannot be definitely determined not to be malignant. At present, it is obvious that VATS should be recommended for operable patients with tumors that are highly suggestive of benign lesions but that cannot be definitely determined not to be malignant, as VATS gives us pathologic confirmation.

CONCLUSION

In conclusion, in clinically diagnosed Stage I lung cancer patients with a tumor ≤20 mm in diameter, SBRT was reasonably safe in this retrospective study. The clinical implications of the high local control rate depend on the accuracy of clinical/radiologic diagnosis for small lung lesions and are to be carefully evaluated in a prospective study.

REFERENCES

1. Onishi H, Shirato H, Nagata Y, *et al.* Hypofractionated stereotactic radiotherapy (HypoFXSRT) for stage I non-small cell lung cancer: Updated results of 257 patients in a Japanese multi-institutional study. *J Thorac Oncol* 2007;2:S94–S100.
2. Uematsu M, Shioda A, Suda A, *et al.* Computed tomography-guided frameless stereotactic radiotherapy for stage I non-small cell lung cancer: A 5-year experience. *Int J Radiat Oncol Biol Phys* 2001;51:666–670.
3. Nagata Y, Takayama K, Matsuo Y, *et al.* Clinical outcomes of a phase I/II study of 48 Gy of stereotactic body radiotherapy in 4 fractions for primary lung cancer using a stereotactic body frame. *Int J Radiat Oncol Biol Phys* 2005;63:1427–1431.
4. Koto M, Takai Y, Ogawa Y, *et al.* A phase II study on stereotactic body radiotherapy for stage I non-small cell lung cancer. *Radiother Oncol* 2007;85:429–434.
5. Nyman J, Johansson KA, Hulten U. Stereotactic hypofractionated radiotherapy for stage I non-small cell lung cancer—mature results for medically inoperable patients. *Lung Cancer* 2006;51:97–103.
6. Onimaru R, Fujino M, Yamazaki K, *et al.* Steep dose-response relationship for stage I non-small-cell lung cancer using hypofractionated high-dose irradiation by real-time tumor-tracking radiotherapy. *Int J Radiat Oncol Biol Phys* 2008;70:374–381.
7. McGarry RC, Papiez L, Williams M, *et al.* Stereotactic body radiation therapy of early-stage non-small-cell lung carcinoma: Phase I study. *Int J Radiat Oncol Biol Phys* 2005;63:1010–1015.
8. Nishio T, Kunieda E, Shirato H, *et al.* Dosimetric verification in participating institutions in a stereotactic body radiotherapy trial for stage I non-small cell lung cancer: Japan clinical oncology group trial (JCOG0403). *Phys Med Biol* 2006;51:5409–5417.
9. Shaffer K. Role of radiology for imaging and biopsy of solitary pulmonary nodules. *Chest* 1999;116:519S–522S.
10. Libby DM, Henschke CI, Yankelevitz DF. The solitary pulmonary nodule: Update 1995. *Am J Med* 1995;99:491–496.
11. O'Reilly PE, Brueckner J, Silverman JF. Value of ancillary studies in fine needle aspiration cytology of the lung. *Acta Cytol* 1994;38:144–150.
12. Mack MJ, Hazelrigg SR, Landreneau RJ, *et al.* Thoracoscopy for the diagnosis of the indeterminate solitary pulmonary nodule. *Ann Thorac Surg* 1993;56:825–830; discussion 830–822.
13. Gould MK, Maclean CC, Kuschner WG, *et al.* Accuracy of positron emission tomography for diagnosis of pulmonary nodules and mass lesions: A meta-analysis. *J Am Med Assoc* 2001;285:914–924.
14. Jeong SY, Lee KS, Shin KM, *et al.* Efficacy of PET/CT in the characterization of solid or partly solid solitary pulmonary nodules. *Lung Cancer* 2008;61:186–194.
15. Nomori H, Watanabe K, Ohtsuka T, *et al.* Evaluation of F-18 fluorodeoxyglucose (FDG) PET scanning for pulmonary nodules less than 3 cm in diameter, with special reference to the CT images. *Lung Cancer* 2004;45:19–27.
16. Lamy P, Grenier J, Kramar A, *et al.* Pro-gastrin-releasing peptide, neuron specific enolase and chromogranin A as serum markers of small cell lung cancer. *Lung Cancer* 2000;29:197–203.
17. Solaini L, Prusciano F, Bagioni P, *et al.* Video-assisted thoracic surgery (VATS) of the lung: Analysis of intraoperative and postoperative complications over 15 years and review of the literature. *Surg Endosc* 2008;22:298–310.
18. Okada M, Koike T, Higashiyama M, *et al.* Radical sublobar resection for small-sized non-small cell lung cancer: A multicenter study. *J Thorac Cardiovasc Surg* 2006;132:769–775.

Int. J. Radiation Oncology Biol. Phys., Vol. 70, No. 3, pp. 931–934, 2008

0360-3016/08/$–see front matter

ELSEVIER

doi:10.1016/j.ijrobp.2007.10.003

PHYSICS CONTRIBUTION

THREE-DIMENSIONAL INTRAFRACTIONAL MOTION OF BREAST DURING TANGENTIAL BREAST IRRADIATION MONITORED WITH HIGH-SAMPLING FREQUENCY USING A REAL-TIME TUMOR-TRACKING RADIOTHERAPY SYSTEM

RUMIKO KINOSHITA, M.D., SHINICHI SHIMIZU, M.D., HIROSHI TAGUCHI, M.D., NORIO KATOH, M.D., MASAHARU FUJINO, M.D., RIKIYA ONIMARU, M.D., HIDEFUMI AOYAMA, M.D., FUMI KATOH, M.D., TOKUHIKO OMATSU, M.D., MASAYORI ISHIKAWA, PH.D., AND HIROKI SHIRATO, M.D.

Department of Radiology, Hokkaido University School of Medicine, Sapporo, Japan

Purpose: To evaluate the three-dimensional intrafraction motion of the breast during tangential breast irradiation using a real-time tracking radiotherapy (RT) system with a high-sampling frequency.

Methods and Materials: A total of 17 patients with breast cancer who had received breast conservation RT were included in this study. A 2.0-mm gold marker was placed on the skin near the nipple of the breast for RT. A fluoroscopic real-time tumor-tracking RT system was used to monitor the marker. The range of motion of each patient was calculated in three directions.

Results: The mean ± standard deviation of the range of respiratory motion was 1.0 ± 0.6 mm (median, 0.9; 95% confidence interval [CI] of the marker position, 0.4–2.6), 1.3 ± 0.5 mm (median, 1.1; 95% CI, 0.5–2.5), and 2.6 ± 1.4 (median, 2.3; 95% CI, 1.0–6.9) for the right–left, craniocaudal, and anteroposterior direction, respectively. No correlation was found between the range of motion and the body mass index or respiratory function. The mean ± standard deviation of the absolute value of the baseline shift in the right–left, craniocaudal, and anteroposterior direction was 0.2 ± 0.2 mm (range, 0.0–0.8 mm), 0.3 ± 0.2 mm (range, 0.0–0.7 mm), and 0.8 ± 0.7 mm (range, 0.1–1.8 mm), respectively.

Conclusion: Both the range of motion and the baseline shift were within a few millimeters in each direction. As long as the conventional wedge-pair technique and the proper immobilization are used, the intrafraction three-dimensional change in the breast surface did not much influence the dose distribution.

Breast cancer, Organ motion, Real-time tumor-tracking radiotherapy system, Intrafraction error.

INTRODUCTION

Breast conservation therapy, lumpectomy, and whole breast radiotherapy (RT) have been accepted as the standard treatment for early-stage breast carcinoma on the basis of trials comparing breast conservation therapy with mastectomy (1, 2). After breast conservation surgery, the breast is irradiated with lateral and medial tangential fields using the wedge-pair technique. Detailed observations of breast motion have been made during RT using two-dimensional (2D) portal imaging systems (3, 4). The portal image represents the relationship between the breast and radiation field but does not have sufficient information about the three-dimensional (3D) motion of the breast tissue. Recently, complicated treatment methods such as the dynamic wedge method, intensity-modulated RT, and partial breast RT have been introduced for breast RT (5–8). The 3D intrafraction motion of the breast has been given a lot of attention in response to the introduction of these technologies.

The purpose of this study was to evaluate the 3D intrafraction magnitudes of respiratory motion of the breast precisely with a high-sampling frequency. Our hope is that the results of this study will provide the basic data needed to calculate an appropriate internal margin in each direction for precise irradiation using a 3D treatment planning system.

METHODS AND MATERIALS

A total of 17 patients who received breast conservation treatment were included in this study. The median age was 58 years (range, 37–76). In 16 of 17 patients whose weight and height were available, the mean ± standard deviation (SD) of the body mass index [BMI] was 22.0 ± 2.6 kg/m^2. One of the women had malignant lymphoma

Reprint requests to: Hiroki Shirato, M.D., Department of Radiology, Hokkaido University School of Medicine, North-15 West-7, Sapporo, Japan. Tel: (81) 11-706-5974; Fax: (81) 11-706-7876; E-mail: hshirato@radi.med.hokudai.ac.jp

Presented in part at the 48th Annual Meeting of the American Society of Therapeutic Radiology and Oncology (ASTRO), November 5–9, 2006, Philadelphia, PA.

Funded by a Grant-in-Aid from the Ministry of Education Culture, Sports, Science, and Technology of Japan.

Conflict of interest: none.

Received May 17, 2007, and in revised form Oct 1, 2007. Accepted for publication Oct 2, 2007.

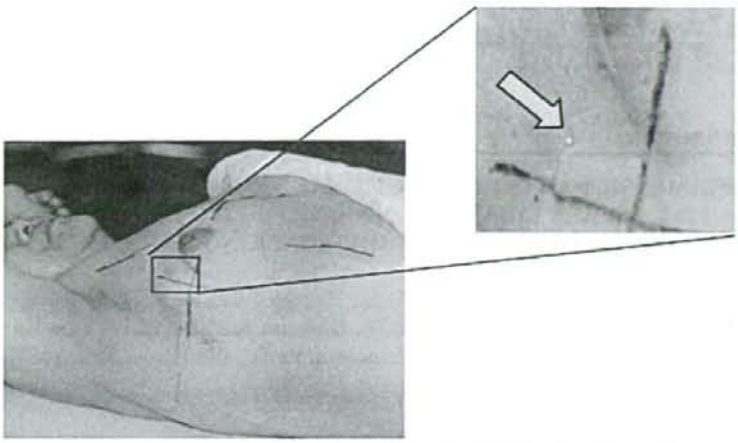

Fig. 1. Gold marker (2 mm) placed on skin near nipple (broad arrow) of right breast. Patient in supine position, with ipsilateral arm abducted and immobilized using Moldcare arm rest (Alcare, Tokyo, Japan). Patients were instructed to maintain light, easy breathing during radiotherapy.

and underwent biopsy only. The remainder underwent breast conservation surgery. Of the 17 patients, 12 had right-sided and 5 left-sided breast cancer. All patients provided written informed consent for the additional study using the real-time tracking radiotherapy system.

Each patient was placed in the supine position with the ipsilateral arm abducted and immobilized using a Moldcare arm rest (Alcare, Tokyo, Japan) (9). The Moldcare is a custom-made arm rest that comfortably immobilizes a patient's arm during RT. A 2.0-mm gold marker was placed near the nipple of the breast to be irradiated (Fig. 1). Treatment planning was performed using computed tomography images under normal breathing with a 3-mm slice thickness for the breast region and 7 mm for the rest of the region.

A fluoroscopic real-time tracking system was used to monitor the position of the gold marker. The details of the tracking system have been previously described (10–12). The system consists of four sets of a diagnostic fluoroscope, an image processor unit, a trigger control unit, and an image display unit, as well as a conventional linear accelerator with multileaf collimators. The system was developed to determine the 3D position of a metallic marker on the human body every 0.03 s using two sets of diagnostic fluoroscopy.

In this study, breast motion was evaluated using tracking data from the real-time tumor-tracking RT system. The software used was the same as that used in previous series for lung tumors and the digestive tract (13, 14). In brief, the marker coordinates were used to measure the range (maximum minus minimum) of the marker position. Fluoroscopic imaging of the breast motion was taken for 1 min. During the fluoroscopic examination, 95% of the marker position was within the border of the original marker position. The Wilcoxon signed rank test was used to compare the range of motion in each direction (right–left [R–L], craniocaudal [CC], and anteroposterior [AP]). A p value <0.05 was considered statistically significant. Regression analysis was performed between the range of motion in the AP direction and BMI (weight in kilograms divided by the height in square meters).

In 10 of 17 patients who underwent examination of respiratory function, regression analysis was performed between the range of motion in the AP and two parameters of respiratory function as follows:

$$\%VC = \text{actual VC/predicted VC} \times 100$$
$$FEV_1\% = FEV_1/\text{FVC (forced VC)} \times 100$$

where %VC is the ratio of vital capacity, VC is the vital capacity, $FEV_1\%$ is the ratio of forced expiratory volume in 1 s, and FVC is the forced VC. We also calculated the baseline shift during 1 min using linear regression fitting of the breast motion data.

RESULTS

Respiratory motion range

The mean ± SD of the range of motion of the breast was 1.0 ± 0.6 mm (median, 0.9; 95% confidence interval [CI] of the marker position, 0.4–2.6), 1.3 ± 0.5 mm (median, 1.1; 95% CI, 0.5–2.5), and 2.6 ± 1.4 mm (median, 2.3; 95% CI 1.0–6.9) for the R–L, CC, and AP direction, respectively. The range of motion was the largest in the AP direction in all patients. The range of motion was the smallest in the R–L direction in 15 of 17 patients. Figure 2 shows the range of respiratory motion for each patient in the R–L, CC, and AP directions. The range of motion in the AP direction was statistically greater than that in the other directions (AP vs. R–L, $p = 0.0003$, and AP vs. CC, $p = 0.0003$, Wilcoxon signed rank test; Fig. 3). The mean ± SD of the range of motion of the right breast was 1.2 ± 0.6, 1.5 ± 0.5, and 3.1 ± 1.4 mm for the R–L, CC, and AP direction, respectively. The mean ± SD of the range of motion of the left breast was 0.7 ± 0.6, 0.9 ± 1.0, and 1.4 ± 1.2 mm for the R–L, CC, and AP directions, respectively.

Regression analysis

No correlation was apparent between the range of motion in the AP direction and the BMI. The body weight range was

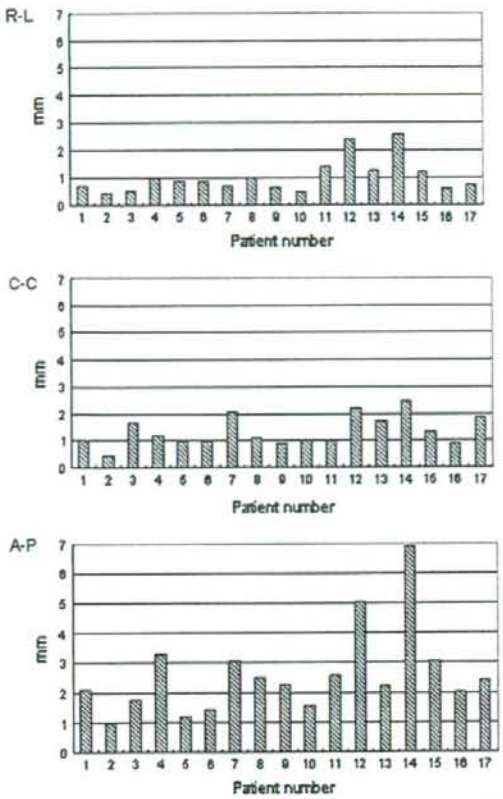

Fig. 2. Range of respiratory motion of each patient along right–left (R-L), craniocaudal (C-C), and anteroposterior (A-P) axis.

42–61.5 kg, and body height range was 146–167 cm. Also, no correlation was found between the range of motion in the R–L and CC directions and BMI. For the 10 women with respiratory function data available, the mean ratio of the vital capacity and ratio of the forced expiratory volume in 1 s was 123.5% ± 21.7% (range, 67.9–143.1%) and 120.3% ± 24.1% (range, 64.5–146.7%), respectively. These parameters did not correlate with the range of respiratory motion in the AP direction.

Baseline shift

No subject had >1 mm baseline shift in the R–L or CC directions; however, 4 patients had a >1 mm baseline shift in the AP direction (Fig. 4). Two patients had no apparent baseline shift in the R–L direction, and two had no apparent baseline shift in the AP direction. The mean ± SD of the absolute value of the baseline shift in the R–L, CC, and AP direction was 0.2 ± 0.2 mm (range, 0.0–0.8 mm), 0.3 ± 0.2 mm (range, 0.0–0.7 mm), and 0.8 ± 0.7 mm (range, 0.1–1.8 mm), respectively.

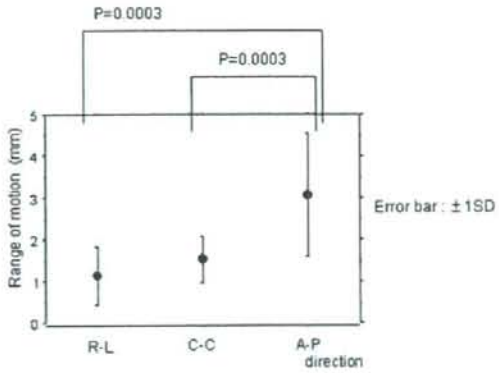

Fig. 3. Mean and standard deviation of range of respiratory motion along right–left (R-L), craniocaudal (C-C), and anteroposterior (A-P) axis.

DISCUSSION

Fein *et al.* (3) and Smith *et al.* (4) used an electronic on-line portal imaging system with a 2D beam's eye view. The beam's eye view represents the relationship between the breast and the radiation field; however, it is not suitable for investigating the 3D motion of the breast tissue. The present on-line portal imaging system can acquire 30–60 images/min. We monitored using a greater sampling frequency, 30 times/s, using a real-time tracking RT system, which potentially has more accuracy in detecting finite motion.

Fein *et al.* (3) have shown that 2D intrafraction movement of the breast resulted in CC motion (described as the interior central margin in their report) of 0.85 mm (range, 0.1–3.2 mm) and motion tangential to the beam axis (the central breast distance in their report) of 2.1 mm (range, 0.4–19 mm). The 2D data of their study were compatible with our 3D findings of a mean ± SD of 1.3 ± 0.5 mm (range, 0.5–2.5 mm), 2.6 ± 1.4 mm (range, 1.0–6.9 mm), and 1.0 ± 0.6 mm (range, 0.4–2.6 mm) in the CC, AP, and R–L direction, respectively. In our study, the motion of the breast in the AP direction was significantly greater than that in the R–L direction. Therefore, our results suggest that the relatively large intrafraction motion tangential to the beam axis in the

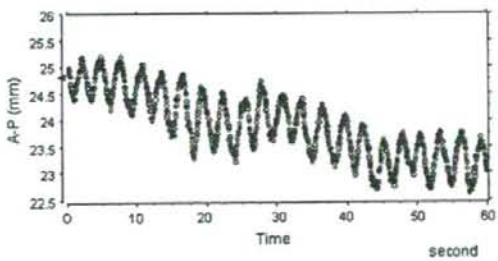

Fig. 4. Example of baseline shift in anteroposterior (A-P) direction during 60 min.

study by Fein *et al.* (3) mainly resulted from the motion of the breast in the AP direction rather than in the R–L direction.

We have speculated that obesity might be related to the amplitude of surface marker movement on the breast and measured the BMI. However, we found no predictive value between the range of motion of the breast and BMI, at least in our data from relatively thin Japanese women. No predictive value was found between the range of motion of surface markers on the breast and the respiratory function tests, ratio of vital capacity and ratio of forced expiratory volume in 1 s. This is consistent with our previous analysis of motion during RT for lung cancer, in which we did not find any significant correlation between respiratory function and the magnitude of marker movement in any direction (15).

We did not examine the interfraction uncertainty of tangential breast RT in this study, because we found that maintaining the gold marker on the chest wall during RT was no better than using a tattoo on the skin surface as a surrogate. Fein *et al.* (3) and Smith *et al.* (4) have shown that intrafractional changes of the irradiated lung area were much smaller than the interfraction changes of the lung area on electronic portal imaging during tangential field breast RT. We agree that the intrafractional changes on the breast surface are usually only a few millimeters and should not influence the dose distribution very much.

Seppenwoolde *et al.* (16) have already shown that a baseline shift often occurs in the position of the internal fiducial marker in lung cancer patients. They demonstrated that the direction of the shift was largest in the AP direction. We also found the baseline shift in the position of the surface marker on the skin to be mainly in the AP direction. The time trends could be attributed to patient relaxation throughout the treatment or to gravity acting on breast tissue shortly after the patient was placed in the supine position with one arm held overhead. When the conventional wedge-pair technique with the Moldcare arm rest was used, the baseline shift was <2 mm, and often <1 mm; therefore, we concluded that we did not need to be concerned about the baseline shift. Even in intensity-modulated RT or focused partial RT for breast cancer, gated RT or close observation during RT might not be beneficial in most patients in terms of the intrafractional movement. However, for intensity-modulated RT, with a longer treatment time, or for poor treatment positioning techniques without proper armrest equipment, the intrafractional movement and baseline shift have the potential to increase the intrafractional dislocation. Gated RT or close observation during RT, not fluoroscopic but optical, might be useful for these situations. Recent sophisticated methods such as 3D relocation of the breast using multiple surface markers and infrared optical beams might be useful for reducing the interfraction setup error (17).

Real-time tumor tracking RT systems inevitably use diagnostic X-rays for the observation during RT. For breast RT, optical observation of the skin surface is more appropriate because it foregoes excessive X-ray exposure. Real-time tracking RT is not used for breast RT in routine practice, but the lessons from this study should be useful for contouring the internal target volume in a hospital setting.

REFERENCES

1. Veronesi U, Cascinelli N, Mariani L, *et al.* Twenty-year follow-up of a randomized study comparing breast-conserving surgery with radical mastectomy for early breast cancer. *N Engl J Med* 2002;347:1227–1232.
2. Fisher B, Anderson S, Bryant J, *et al.* Twenty-year follow-up of a randomized trial comparing total mastectomy, lumpectomy, and lumpectomy plus irradiation for the treatment of invasive breast cancer. *N Engl J Med* 2002;347:1233–1241.
3. Fein D, McGee KP, Schultheiss T, *et al.* Intra- and interfractional reproducibility of tangential breast fields: A prospective on-line portal imaging study. *Int J Radiat Oncol Biol Phys* 1996;34:733–740.
4. Smith R, Bloch P, Harris E, *et al.* Analysis of interfraction and intrafraction variation during tangential breast irradiation with an electronic portal imaging device. *Int J Radiat Oncol Biol Phys* 2005;62:373–378.
5. Sidhu S, Shdhu N, Papointe C, *et al.* The effects of intrafraction motion on dose homogeneity in a breast phantom with physical wedges, enhanced dynamic wedges, and ssIMRT. *Int J Radiat Oncol Biol Phys* 2006;66:64–75.
6. Leavitt D. New application of enhanced dynamic wedge for tangent breast irradiation. *Med Dosim* 1997;22:247–251.
7. Kestin L, Sharpe M, Frazier R, *et al.* Intensity modulation to improve dose uniformity with tangential breast radiotherapy: Initial clinical experience. *Int J Radiat Oncol Biol Phys* 2000; 48:1559–1568.
8. Formenti S, Rosenstein B, Skinner K, *et al.* T1 stage breast cancer: Adjuvant hypofractionated conformal radiation therapy to tumor bed in selected postmenopausal breast cancer patients—Pilot feasibility study. *Radiology* 2002;22:171–178.
9. Kitahara T, Shirato H, Nishioka T, *et al.* A new mold material for customized patient positioning in radiotherapy. *Radiother Oncol* 1998;47:77–79.
10. Shirato H, Shimizu S, Shimizu T, *et al.* Real-time tumor-tracking radiotherapy. *Lancet* 1999;353:1331–1332.
11. Shirato H, Shimizu S, Kitamura K, *et al.* Four-dimensional treatment planning and fluoroscopic real-time tumor tracking radiotherapy for moving tumor. *Int J Radiat Oncol Biol Phys* 2000;48:435–442.
12. Shirato H, Shimizu S, Kunieda T, *et al.* Physical aspects or a real-time tumor tracking system for gated radiotherapy. *Int J Radiat Oncol Biol Phys* 2000;48:1187–1195.
13. Shimizu S, Shirato H, Ogura S, *et al.* Detection of lung tumor movement in real-time tumor-tracking radiotherapy. *Int J Radiat Oncol Biol Phys* 2001;51:304–310.
14. Hashimoto T, Shirato H, Kato M, *et al.* Real-time monitoring of a digestive tract marker to reduce adverse effects of moving organs at risk (OAR) in radiotherapy for thoracic and abdominal tumors. *Int J Radiat Oncol Biol Phys* 2005;61:1559–1564.
15. Onimaru R, Shirato H, Fujino M, *et al.* The effect of tumor location and respiratory function on tumor movement estimated by real-time tracking radiotherapy (RTRT) system. *Int J Radiat Oncol Biol Phys* 2005;63:164–169.
16. Seppenwoolde Y, Shirato H, Kitamura K, *et al.* Precise and real-time measurement of 3D tumor motion in lung due to breathing and heartbeat, measured during radiotherapy. *Int J Radiat Oncol Biol Phys* 2002;53:882–834.
17. Spadea MF, Baroni G, Riboldi M, *et al.* Patient set-up verification by infrared optical localization and body surface sensing in breast radiation therapy. *Radiother Oncol* 2006;79:170–178.